Estimation of Manning's Roughness Coefficient Distribution for Hydrodynamic Model Using Remotely Sensed Land Cover Features

A. K. M. Azad Hossain, Yafei Jia and Xiabo Chao
National Center for Computational Hydroscience and Engineering
The University of Mississippi
Carrier Hall 102, University, MS 38677
ahossain@ncche.olemis.edu

Abstract— **This research explores the potential of remote sensing techniques to derive distributed Manning's roughness coefficient (Manning's *n*) for the use in hydrodynamic models for numerical simulation of open channel flow in natural channels and flood plains. Normalized Difference Vegetation Index (NDVI) based land use land cover (LU/LC) data was generated using the Landsat 5 Thematic Mapper (TM) and Advance Land Observing Satellite (ALOS) Panchromatic Remote-sensing Instrument for Stereo Mapping (PRISM) imagery. Manning's *n* were obtained from published literature for different features in flood plains and correlated with the remote sensing derived LU/LC features. CCHE2D model, developed by the National Center for Computational Hydroscience and Engineering (NCCHE), at The University of Mississippi, for simulating two dimensional depth-averaged unsteady flow and sediment transport was used to validate the remote sensing derived distributed Manning's *n* for channel flow calculation. Results obtained from this research indicate that satellite imagery derived LU/LC data has potential to be used to improve hydrodynamic model simulation by providing distributed Manning's roughness coefficient for respective model domains.**

Keywords*-Manning's roughness coefficient; Remote sensing; Land use land cover; CCHE2D model.*

I. INTRODUCTION

Manning's roughness coefficient (Manning's *n*) is one of the most important empirical parameters in the field of hydrology, hydraulics and other surface water flow related science and engineering, which quantifies the resistance of the bed to the flow of water and is used for open channel flow calculation in natural channels and flood plains. For simple calculation of flow velocity Manning's equation is expressed as equation [1].

$$V = \frac{1}{n} R^{2/3} S^{1/2} \quad (1)$$

V = Flow velocity, n = Manning's roughness coefficient, R = Hydraulic radius, S = Channel slope

When surface flows are modeled solving shallow water differential equations, the shear stress term is often modeled as equation [2].

$$\frac{\tau}{\rho} = g \frac{n^2 V^2}{R^{1/3}} \quad (2)$$

τ = shear stress, ρ = water density, g = acceleration due to gravity.

Suggested values for Manning's *n,* according to factors that affect roughness, are found in number of articles including [4], [5], [12], [13], and [14]. Although much research has been done to determine roughness coefficients for open-channel flow [10], less has been done for densely vegetated flood plains, coefficients for which are typically very different from those for channels. There is a tendency to regard the selection of roughness coefficients as either an arbitrary or an intuitive process and traditionally hydrodynamic models get the input of Manning's *n* manually estimated based on visual interpretation of the available land cover information for the model domain. This approach is particularly difficult to carry out for a large computational area with various land uses, and will bring a high degree of uncertainties in the model simulation results.

In this research it is attempted to (1) correlate the remotely sensed vegetation index (VI) based land cover features with pre-estimated Manning's *n*, (2) convert the land cover information into a raster layer with distributed Manning's *n*, (3) validate the remote sensing derived Manning's *n* using observed data, and (4) use the raster layer in the hydrodynamic model simulation.

II. STUDY SITE AND SATELLITE DATA USED

Midwest USA affected by a 500 year flood in June 2008. More than 51 counties in 5 states (MO, IL, IA, WI and MN) were flooded. This research used Mississippi River and its associated flood plains (inundated by Midwest flood) around Alexandria, MO and Warsaw, IL areas as the study site (Figure 1). Landsat 5 Thematic Mapper (TM) imagery acquired on April 29, 2008 at 30 m resolution was used to generate the land use land cover map of the study site. Advance Land Observing Satellite (ALOS) Panchromatic

Remote-sensing Instrument for Stereo Mapping (PRISM) imagery acquired on July 07, 2008 at 2.5 m resolution was used to delineate the levee line along the Mississippi River (Figure 1).

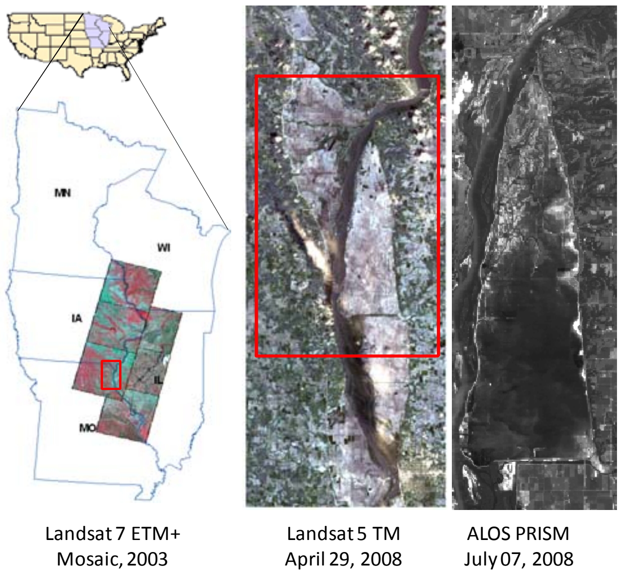

Figure 1. Location of study site and satellite data used

III. Methods and Results

A. Image Processing Techniques

The Iterative Self-Organizing Data Analysis Technique (ISODATA), Normalized Difference Vegetation Index (NDVI) and Density Slicing technique were used to generate the land use land cover data for the study site.

1) ISODATA Clustering Algorithm: The Iterative Self-Organizing Data Analysis Technique (ISODATA) [7] is an iterative unsupervised classification scheme [11]. This algorithm minimizes the within cluster variability and categorizes the pixels into number of classes based on statistics. The objective function is the sums of squares distances between each pixel and its assigned cluster center. Minimizing the $SS_{distances}$ is equivalent to minimizing the Mean Squared Error (*MSE*). The *MSE* is a measure of the within cluster variability.

$$SS_{distances} = \sum_{\forall x} [x - C(x)]^2 \quad (3)$$

$$MSE = \frac{\sum_{\forall x} [x - C(x)]^2}{(N-c)b} = \frac{SS_{distances}}{(N-c)b} \quad (4)$$

C(x) = the mean of the cluster that pixel *x* is assigned to, *N* is the number of pixels, *c* indicates the number of clusters, and *b* is the number of spectral bands.

2) Normalized Difference Vegetation Index (NDVI)

The Normalized Difference Vegetation Index (NDVI) [3] is a simple numerical indicator, one of the most widely accepted and used vegetation indices [8]. NDVI can be used as an indicator of relative biomass and greenness [9]. It uses the high reflectance values of vegetation in the Near Infrared (NIR) region and low values of reflectance in the red region. NDVI is based on a ratio of the NIR and the red bands.

$$NDVI = \frac{(NIR - R)}{(NIR + R)} \quad (5)$$

NDVI values for a given pixel range from -1 to +1. A zero means no vegetation and close to +1 (0.8 - 0.9) indicates the highest possible density of green leaves.

3) Density Slicing: Density slicing is a digital data interpretation method used in analysis of remotely sensed imagery to enhance the information gathered from an individual brightness band [6]. Density slicing is done by dividing the range of brightness in a single band into intervals, then assigning each interval to a color [1] to represent specific classes.

B. Land use land cover (LU/LC) data generation

Normalized Difference Vegetation Index (NDVI) was calculated using the Landsat 5 Thematic Mapper (TM) imagery and classified into different land use land cover (LU/LC) features according to the vegetation density in the flood plains and islands in river channels. The land use land cover (LU/LC) classes including natural stream, trees, heavy brush, light brush, pasture/farmland, bare earth, urban areas(concrete finished), roads/highways (asphalt) and levees (gravelly surface) (Figure 2). The classification threshold values were determined by density slicing techniques using the thematic clusters derived from unsupervised classification scheme using the ISODATA clustering algorithm. Roads/highways and levees were delineated using the acquired high resolution ALOS PRISM imagery and incorporated with the Landsat derived LU/LC data using GIS.

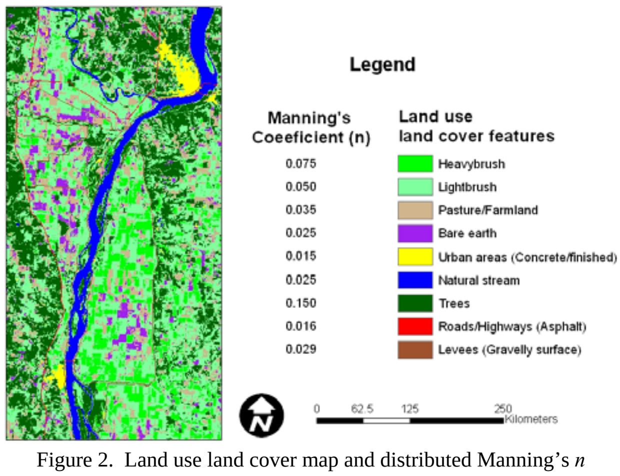

Figure 2. Land use land cover map and distributed Manning's *n*

C. Correlation of Manning's Roughness Coefficient

Manning's roughness coefficient values (Manning's *n*) for each of the remote sensing derived land cover features within the channel and associated floodplains were obtained from published literature including [4], [5], [12], [13], [14].

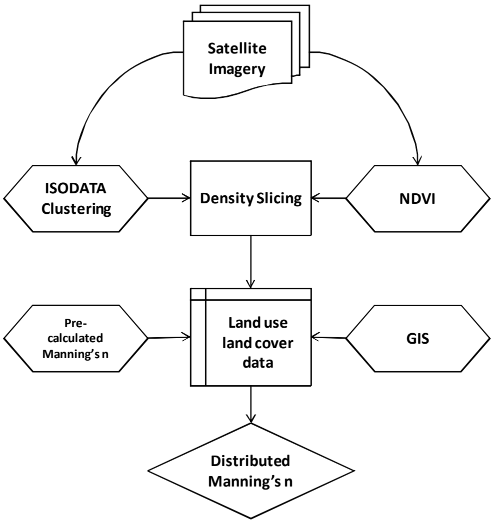

Figure 3. Process of obtaining distributed Manning's *n*

The obtained Manning's *n* values were assigned to each corresponding land cover features in the LU/LC raster layer generated by image processing techniques. The Manning's *n* values were assigned using GIS and the LU/LC thematic data were converted into the distributed Manning's *n* thematic data. Figure 2 shows the land use land cover map and corresponding distributed Manning's *n* values. Figure 3 shows the flow chart of obtaining distributed manning's *n* using satellite imagery.

D. Numerical Simulations

CCHE2D model, developed by the National Center for Computational Hydroscience and Engineering (NCCHE), at The University of Mississippi [15], for simulating two dimensional depth-averaged unsteady flow and sediment transport [16] was used to simulate flooding in the Mississippi River around Alexandria, MO and Warsaw, IL areas from June 16, 2008 to June 21, 2008 (Figure 4). The remote sensing derived Manning's roughness coefficient (Manning's *n*) obtained in this study was used in the flood simulation (Figure 4). The simulation result was compared with satellite observed flood extent maps and was found in good agreement [2].

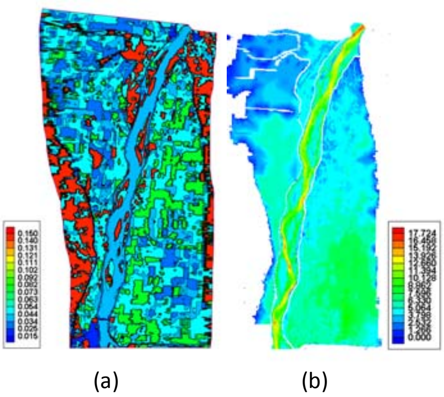

Figure 4. Distributed Manning's *n* for the study site and CCHE2D flow simulation results

E. Validation of RS derived Manning's n

Since measured data in the flooded area (flood plain) was not available a subset of the study site, the Mississippi River main channel, was used as the model domain for the validation of remote sensing derived Manning's *n* in flow simulation. The model domain includes Mississippi River between Lock and Dam 19 and 20 (Figure 6a). From the river engineering experience, Manning's *n* for the channel flow in this research should be about 0.025 and this value is assigned for the flow area with river sediments. For areas covered with vegetations such as, islands and point bars, the Manning's *n* should be higher and have a larger resistance to the flow. If 0.025 is used everywhere including vegetated areas, the overall flow resistance would be too low. However, it would be too time consuming and less accurate to specify a distributed field of Manning's *n* manually. In this study, distributed Manning's *n* is obtained by using remote sensing data of land use and land cover to enhance the modeling accuracy and efficiency. The obtained data was validated using measured hydrology data (Figure 5) and computational model.

Channel flow was simulated using CCHE2D model for several low flow and high flow conditions of the river (Figure 5). Flow was computed using both constant Manning's *n* (n = 0.025) and remote sensing derived distributed Manning's *n*. Water surface elevation computed in this way for Lock and Dam 19 (upstream) was compared with the measured water surface elevation at the Lock and Dam. Figure 6 shows the initial bed elevation within the model domain (a), remote sensing derived distributed Manning's n used in flow computation (b) and an example of CCHE2D flow simulation (c). Figure 7 shows the comparison of the computed water surface elevations with the measured water surface elevation at Lock and Dam 19. Table I provides the computed and measured water surface elevations and discharge at Lock and Dam 19.

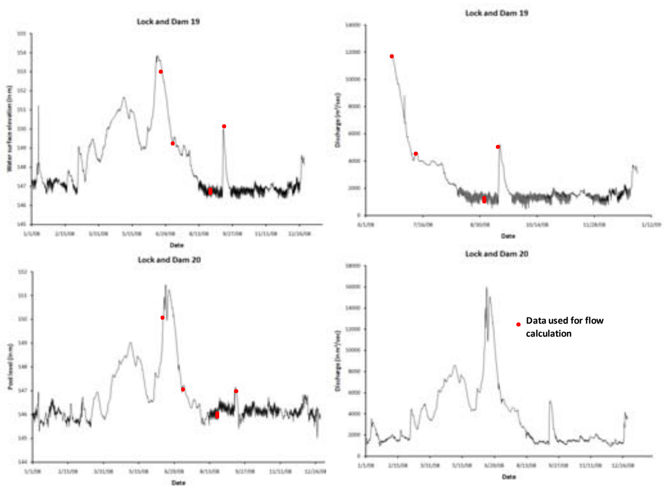

Figure 5. Hydrographs at Lock and Dam 19 and 20

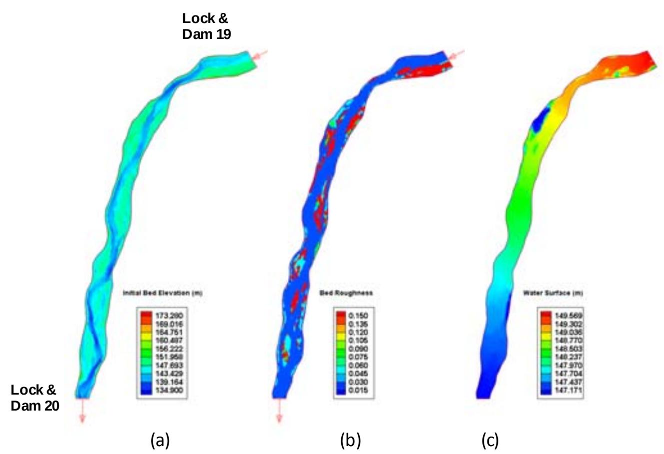

Figure 6. CCHE2D flow simulation for validation of remote sensing derived distributed manning's roughness coefficient validation (a) model domain, (b) Manning's *n* and (c) flow simulation results.

TABLE I. COMPUTED AND MEASURED WATER SURFACE ELEVATIONS AND DISCHARGE AT LOCK AND DAM 19

Observed Discharge, Q (m^3/sec)	Observed Water Surface Elevation, S_{obs} (m)	Computed Water Surface Elevation, S_{comp}	
		Constant n (= 0.025)	Remote sensing derived n
922.11	146.50	146.57	146.56
1113.39	146.62	146.87	146.88
1162.86	146.65	147.05	147.05
4314.16	149.39	149.55	149.57
5216.61	150.03	150.09	150.12
11791.14	153.59	153.20	153.68

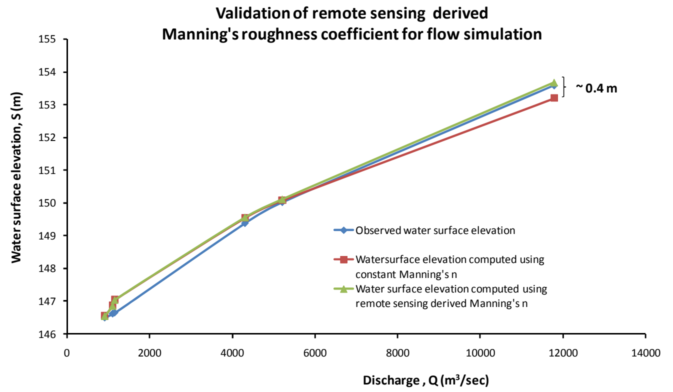

Figure 7. Comparison of the computed water surface elevations with the measured water surface elevation at Lock and Dam 19

IV. DISCUSSION AND CONCLUSION

The comparison between the computed and measured water surface elevations at Lock and Dam 19 shows that at flow conditions (low flow), Q < 2000 m^3/sec and Q> 4000 m^3/sec and < 7000 m^3/sec the computed water surface elevations are in very good agreement with the measured water surface elevation (Table I and Figure. 6). It is observed for computations done by using both constant Manning's *n* and distributed Manning's *n* derived by remote sensing. In flow condition, Q > 2000 m^3/sec and < 4000 m^3/sec the water surface elevations computed by constant Manning's *n* and distributed Manning's *n* are in very good agreement, but both vary from the measured water surface elevations. At flow condition (high flow), Q> 7000 m^3/sec water surface elevation computed by using remote sensing derived distributed Manning's *n* has very good agreement with the measured water surface elevation (Table I and Figure 7). Water surface elevation computed by using constant Manning's *n* is almost 40 cm off from the measured water surface elevation (Table I and Figure 7).

This research is in initial stage and the preliminary results indicate that land use land cover data generated by remote sensing techniques has potential to be used to assign distributed manning's roughness coefficient (Manning's *n*) for numerical calculation of surface water flows. This research also indicates that the accuracy of channel flow calculation using remote sensing derived distributed Manning's *n* is higher than that obtained by using constant Manning's *n*.

REFERENCES

[1] A. Hossain, and G. Easson, "Mapping small reservoirs in semi-arid region using optical and microwave remote sensing", Proceedings of ASPRS 2007 Annual Conference,Tampa, Florida, USA, May 7-11,2007.

[2] A. Hossain, X. Chao, and Y. Jia, "Mapping 2008 Midwest Flood Dynamics Using Multi-sensor Remotely Sensed Data, a case study of CCHE2D Flood Simulation Results Validation", MAESC 2009 Conference, Christian Brothers University, Memphis, TN, May 5, 2009.

[3] F. J. Kriegler, W. A. Malila, R. F. Nalepka, and W. Richardson, "Preprocessing, transformations and their effects on multispectral recognition", Proceedings of the Sixth International Symposium on Remote Sensing of Environment, University of Michigan, Ann Arbor, MI, pp. 97-131, 1969.

[4] F.M. Henderson, Open-channel flow, New York, MacMillan Publishing Co., Inc., 522 p. 1966.

[5] H.H. Barnes, Jr., Roughness characteristics of natural channels, U.S. Geological Survey Water-Supply Paper 1849, 213 p, 1967.

[6] J.B. Campbell, Introduction to Remote Sensing, 3rd ed. Taylor and Francis, London, 2002.

[7] J.R. Jensen, Remote Sensing of the Environment: An Earth Resource Perspective".2nd ed.,Upper Saddle River, NJ: Prentice Hall, 592p, 2007.

[8] J.W. Rouse, R.H. Haas, J.A. Schell, and D.W. Deering, "Monitoring vegetation systems in the Great Plains with ERTS", Third ERTS Symposium, NASA SP-351 I., pp. 309-317, 1973.

[9] R. B. Boone, K. A. Galvin, and S.J. Lynn, "Generalizing El Nino effects upon Maasai livestock using hierarchical clusters of vegetation patterns", Photogrammetric Engineering & Remote Sensing, vol. 66, pp.737-744, 2000.

[10] R.W. Carter, H.A. Einstein, Hinds, Julian, R.W. Powell, and E. Silberman, "Friction factors in open channels, progress report of the task force on friction factors in open channels of the Committee on Hydro-mechanics of the Hydraulics Division", Proceedings, American Society of Civil Engineers, Journal of the Hydraulics Division, vol. 89, no. HY2, pt. 1, pp. 97-143, 1963.

[11] T.M Lillesand. and R.W. Kiefer, Remote Sensing and Image Interpretation, Fourth ed., John Willey and Sons, Inc., 724p, 2000.

[12] V.L. Streeter, Fluid mechanics, New York, McGraw-Hill Book Co., 5th ed. 705p, 1971.

[13] V.T. Chow, Open-channel Hydraulics, New York, McGraw- Hill Book Co., 680p, 1959.

[14] W. H. Graf, Hydraulics of Sediment Transport, Water Resources Publications LLC., 513p, 1998.

[15] Y. Jia, and S.S.Y. Wang, "Numerical model for channel flow and morphological change studies", Journal of Hydraulic Engineering, ASCE, vol.125, no. 9, pp.924-933, 1999.

[16] Y. Jia, S.Y.Y.Wang, and Xu.Yichen, "Validation and application of a 2D model to channels with complex geometry", International Journal of Computational Engineering Science, vol. 3, no. 1, pp. 57-71. 2002.